

# Cardiac Motion Estimation using a ProActive Deformable Model: Evaluation and Sensitivity Analysis

Ken C. L. Wong<sup>1</sup>, Florence Billet<sup>1</sup>, Tommaso Mansi<sup>1</sup>, Radomir Chabiniok<sup>2</sup>,  
Maxime Sermesant<sup>1,3</sup>, Hervé Delingette<sup>1</sup>, and Nicholas Ayache<sup>1</sup>

<sup>1</sup>INRIA, Asclepios project, 2004 route des Lucioles, Sophia Antipolis, France

<sup>2</sup>INRIA, Macs project, Rocquencourt, Le Chesnay, France

<sup>3</sup>King's College London, St Thomas Hospital,  
Division of Imaging Sciences, London, UK

**Abstract.** To regularize cardiac motion recovery from medical images, electromechanical models are increasingly popular for providing *a priori* physiological motion information. Although these models are macroscopic, there are still many parameters to be specified for accurate and robust recovery. In this paper, we provide a sensitivity analysis of a proactive electromechanical model-based cardiac motion tracking framework by studying the impacts of its model parameters. Our sensitivity analysis differs from other works by evaluating the motion recovery through a synthetic image sequence with known displacement field as well as cine and tagged MRI sequences. This analysis helps to identify which parameters should be estimated from patient-specific data and which ones can have their values set from the literature.

## 1 Introduction

Cardiac motion recovery has been an active research area for decades, aiming at accurate and robust estimation of patient-specific myocardial motions from cardiac images. Although medical image modalities, such as magnetic resonance images (MRI), can provide observations of cardiac anatomy and apparent motion, the motion information is often sparse, spatially and temporally noisy, and leads to qualitative rather than quantitative estimations. Therefore, *a priori* motion information is often required to regularize the motion estimation. To this end, electromechanical models have been increasingly popular because of their physiological meaningfulness [1–3].

Macroscopic electromechanical models applied to cardiac image analysis usually consist of three key components: transmembrane potential wave propagation, active contraction forces, and passive biomechanics. Although these models are somewhat simplified compared to cellular cardiac models, they still have many parameters to be specified for clinically relevant recovery. Some authors [4, 5] have already published some sensitivity analyses in which the effects of model parameter variations were quantified on simulated cardiac functions. These studies are useful to assess the relative impact of those parameters, however, without

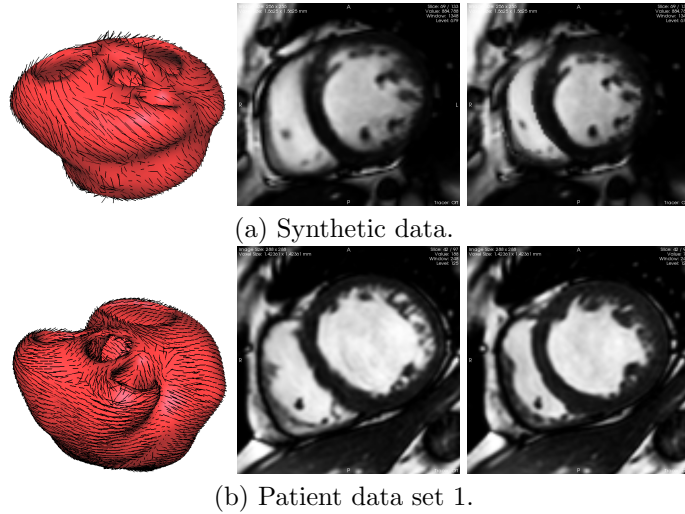


**Fig. 1.** Data used in the experiments. Left to right: heart geometry segmented from patient MRI with synthetic fiber orientations, image frame at the end of diastole, and image frame at the end of systole. For (a), both images were synthesized from the MRI at the mid-diastole with the simulated deformation.

any validation on *in vivo* patient data, the analyses cannot provide any hints about the validity of the model for a given patient.

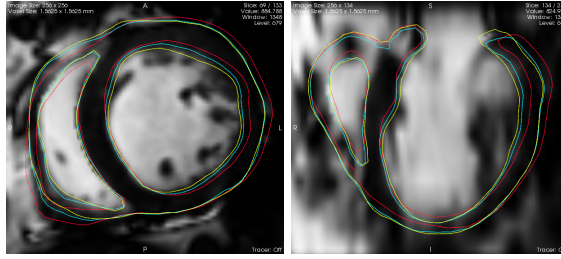
In this paper, we present a sensitivity analysis of electromechanical model parameters for patient-specific cardiac motion recovery from medical images. Through synthetic images for which the ground truth is available, and patient cine MRI for which the corresponding cardiac motion was estimated by experts from tagged MRI, we studied the sensitivity of the motion recovery framework proposed in [1] with respect to the model parameters. This analysis can aid finding which parameters should be estimated from patient-specific measurements and which can have their values set from the literature. It also evaluates the physiological plausibility of the adopted cardiac electromechanical model by comparing the simulated displacements with the expert-estimated motions from the tagged MRI.

## 2 Motion Recovery with Electromechanical Model

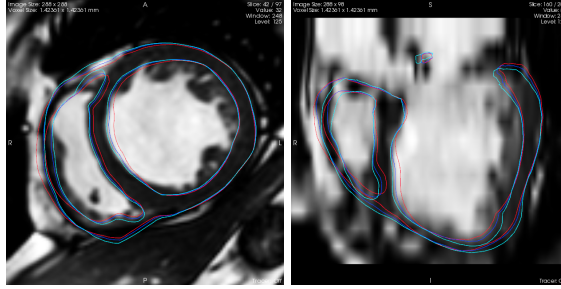
The cardiac motion recovery framework in [1] was tested, which uses the ProActive Deformable Model whose dynamics equation is:

$$\mathbf{M}\ddot{\mathbf{U}} + \mathbf{C}\dot{\mathbf{U}} + \mathbf{K}\mathbf{U} = \mathbf{F}_b + \alpha\mathbf{F}_c + \beta\mathbf{F}_{\text{img}} \quad (1)$$

with  $\mathbf{M}$ ,  $\mathbf{C}$ , and  $\mathbf{K}$  the mass, damping, and stiffness matrices respectively.  $\mathbf{F}_b$  comprises different external loads from boundary conditions.  $\mathbf{F}_c$  and  $\mathbf{F}_{\text{img}}$  are



(a) Synthetic data.



(b) Patient data set 1.

**Fig. 2.** Recovered geometries at the end of systole. Left to right: short-axis and long-axis views of recovered geometries overlapped with images. (a) Yellow line represents the ground truth, and red and cyan lines represent the recovered geometries with the image force scaling parameter  $\beta = 0$  and 45 respectively. (b) Red, blue, and cyan lines represent the recovered geometries with the image force scaling parameter  $\beta = 0, 15,$  and 45 respectively.

the vectors for active contraction forces and image-derived forces respectively.  $\alpha$  and  $\beta$  are scaling parameters involved in the sensitivity analysis.

To obtain the contraction force vector  $\mathbf{F}_c$ , the electrical activation times computed using a multi-front anisotropic Eikonal approach were used to provide the contraction forces along given fiber orientations [6]. The blood pressures on the ventricular walls were provided by prescribed atrial pressures in the filling phase, a three-element Windkessel model in the ejection phase, and ventricular volumetric constraints in the isovolumetric phases. The image force vector  $\mathbf{F}_{\text{img}}$  was computed using a correlation-based 3D block-matching algorithm [7] combined with image intensity gradients, tracking the motions of the salient cardiac features on the heart surfaces. The linear and anisotropic biomechanical properties are included in  $\mathbf{K}$ , whose stiffness is specified by the Young's moduli along and across the fibers ( $E_f, E_{cf}$ ). The sensitivity analysis of cardiac motion recovery can be performed by solving (1) with varying parameters.

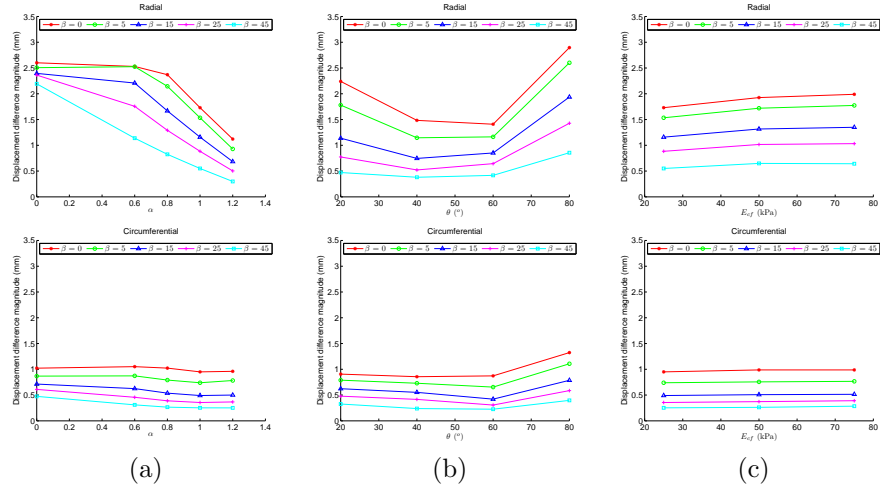


**Fig. 3.** Synthetic data. Displacement difference magnitude versus the change of model parameters at the end of systole. (a) Active force scaling parameter  $\alpha$ . (b) Fiber orientations  $\theta$ . (c) Cross-fiber Young’s modulus  $E_{cf}$ . Different colors encode different values of the image force scaling parameter  $\beta$ .

### 3 Experiments

#### 3.1 Experimental Setup

The sensitivity analysis is focused on parameters related to biomechanics. For each data set, we first obtained a simulation which is similar to the apparent cardiac motion in the images, then we performed cardiac motion recovery with (1) by varying different parameters. The tested parameters include the active force scaling parameter ( $\alpha = 0, 0.6, 0.8, 1.0, 1.2$ ) which controls the amount of myocardial contraction, the image force scaling parameter ( $\beta = 0, 5, 15, 25, 45$ ) which controls the amount of image forces, the Young’s modulus across the fiber direction ( $E_{cf} = 25, 50, 75$  kPa, with  $E_f = 75$  kPa, i.e. from transversely isotropic to isotropic), and with or without ventricular blood pressures as boundary conditions. Different sets of fiber orientations (epicardium to endocardium:  $-\theta$  to  $+\theta$ ,  $\theta = 20^\circ, 40^\circ, 60^\circ, 80^\circ$  for both left and right ventricles) were also tested. We varied only one parameter at a time for each test.

To analyze the sensitivity of the motion recovery framework corresponding to the above parameters, experiments were performed on one synthetic image sequence and two patient cine MRI sequences. No patient electrophysiological data were used during the recoveries.

**Synthetic Data** The synthetic image sequence was obtained through a simulation using the measurements of a patient diagnosed with left bundle branch block. The electromechanical model used in the simulation is highly nonlinear compared with the ProActive Deformable Model used in this analysis. This non-

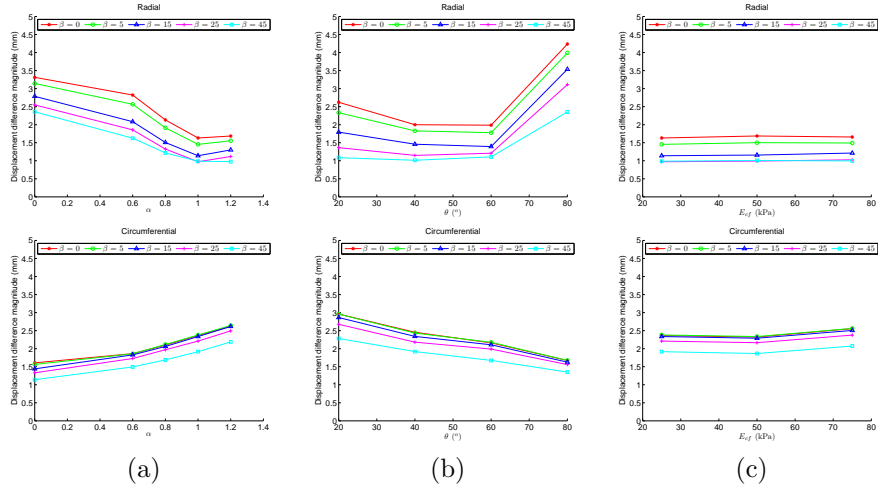


**Fig. 4.** Patient data set 1. Displacement difference magnitude versus the change of model parameters at the end of systole. (a) Active force scaling parameter  $\alpha$ . (b) Fiber orientations  $\theta$ . (c) Cross-fiber Young’s modulus  $E_{cf}$ . Different colors encode different values of the image force scaling parameter  $\beta$ .

linear model uses the Ciarlet-Geymonat material as the nonlinear passive mechanical model and the Bestel-Clement-Sorine model as the active stress model with the consideration of actin-myosin interactions [8]. The anatomical MRI at the mid-diastole was segmented using the semi-automatic segmentation in CardioViz3D [9] to provide the heart geometry including the four basal valvular rings of the ventricles (Fig. 1(a)), with the synthetic fiber orientations generated according to the literature ( $-70^\circ$  to  $+70^\circ$  for the left ventricle, and  $-50^\circ$  to  $+50^\circ$  for the right ventricle). The myocardial electrical activation was simulated using the Eikonal model with the patient electrophysiological data from the LV endocardium. A cycle of cardiac deformation of 1.054 s was simulated. By extrapolating the obtained deformation field to the whole image space, the image from which the heart geometry was segmented was warped into a synthetic image sequence, with 34 ms/frame, and isotropic spatial resolution resolution of 1.5625 mm/voxel. In the sensitivity analysis, the models and pathological situations were assumed to be unknown, thus the parameters used in the ProActive Deformable Model were nominal as described in [1].

**Patient Data** Two cine MRI sequences from patients with dilated cardiomyopathy were used in the experiments. Data set 1 contains a cardiac cycle in 0.87 s, with temporal resolution 29 ms/frame, 10 mm inter-slice spacing, and in-plane resolution 1.42 mm/pixel (Fig. 1(b)). Data set 2 contains a cardiac cycle in 0.73 s, with temporal resolution 25 ms/frame, 10 mm inter-slice spacing, and in-plane resolution 1.45 mm/pixel. Both data sets have corresponding tagged MRI sequences collected at similar time instants, therefore experts could

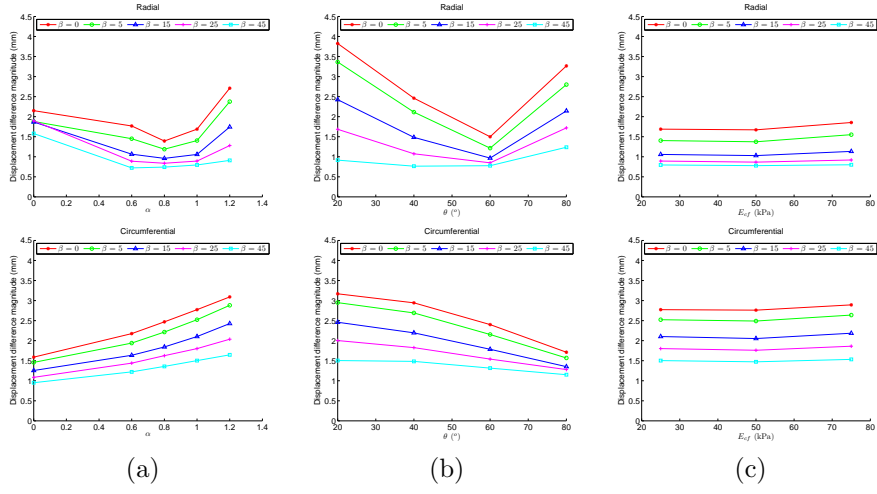


**Fig. 5.** Patient data set 2. Displacement difference magnitude versus the change of model parameters at the end of systole. (a) Active force scaling parameter  $\alpha$ . (b) Fiber orientations  $\theta$ . (c) Cross-fiber Young’s modulus  $E_{cf}$ . Different colors encode different values of the image force scaling parameter  $\beta$ .

perform manual tracking of the tag plane intersections to extract the short-axis myocardial displacements as references. Furthermore, the expert-estimated ejection fractions of data set 1 and 2 are 25% and 15% respectively.

### 3.2 Results and Discussions

The results of the synthetic and patient data were evaluated with the same approach for consistency. For the patient data, as the tagged MRI were not well-registered with the cine MRI, and the tag plane intersections were too sparse to provide meaningful strains from the manually tracked displacements, direct point-to-point comparisons between the recovered deformation and the reference tag motions could not be performed. To cope with this, we compared the regional displacements using the 17 AHA segments [10]. For both recovered and reference motions, the mean radial and circumferential displacements of each segment were computed, which were used to compute the *displacement difference magnitude*:

$$\frac{\sum_i \|\bar{\mathbf{u}}_{\text{recovery}}(i) - \bar{\mathbf{u}}_{\text{reference}}(i)\|}{n} \quad (2)$$

with  $\bar{\mathbf{u}}_{\text{recovery}}(i)$  and  $\bar{\mathbf{u}}_{\text{reference}}(i)$  the mean displacement vectors (radial or circumferential) of the recovered and reference motions in segment  $i$  respectively, and  $n$  the number of segments utilized. As the short-axis tagged MRI cannot provide accurate motions around the apex, only segments 1 to 12 corresponding to the basal and the mid-ventricular levels were used. The results of the synthetic

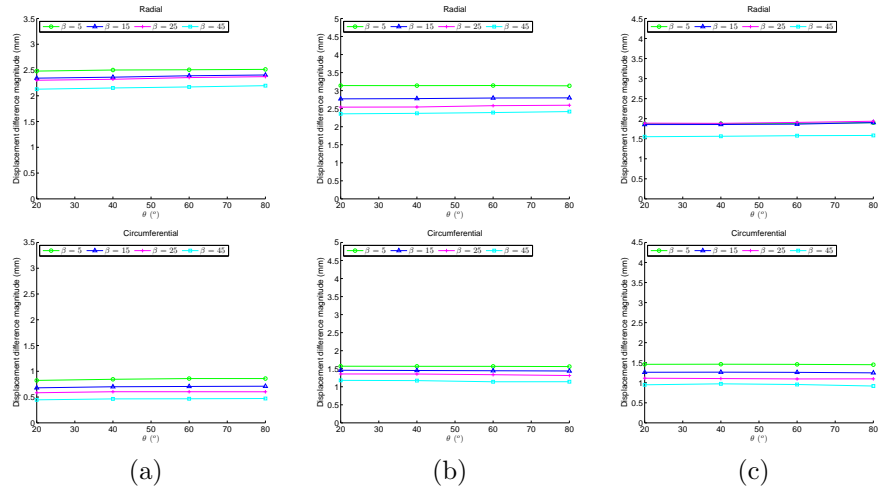


**Fig. 6.** Displacement difference magnitude versus the change of fiber orientations at the end of systole, with the active force scaling parameter  $\alpha = 0$ . (a) Synthetic data. (b) Patient data set 1. (c) Patient data set 2. Different colors encode different values of the image force scaling parameter  $\beta$ .

data were evaluated similarly with the reference motions from the displacement field of the simulated ground truth.

Fig. 2 shows the recovered geometries at the end of systole. For the synthetic data, the heart geometry recovered without image forces (i.e. pure simulation with the ProActive Deformable Model) is quite far from the ground truth, but the one recovered with large image forces is much closer. Interestingly, in some locations such as the endocardium of the left ventricle, the recovered geometry with large image forces is even closer to the apparent heart surfaces than the simulated ground truth. This shows that the recovery framework is capable of correcting imperfectness of initial segmentation by using image intensity gradients. Similarly, for the patient data sets, the larger the image forces, the more subject-specific the recovered geometries.

Fig. 3, 4, 5, and 7 show the changes of the displacement difference magnitude versus the changes of model parameters under different image forces. Similar to the observations in Fig. 2, in all tests, the larger the image forces, the closer the recovered motions to the reference motions. Furthermore, in most cases, the image forces show greater influences on the radial displacements rather than the circumferential displacements. This is reasonable as cine MRI, different from tagged MRI, can mainly provide apparent radial motions of the myocardium instead of circumferential motions.

Comparing the sensitivities between parameters, the anisotropy of mechanical stiffness is the least sensitive (Fig. 3, 4, and 5). The displacement difference magnitudes show relatively small changes when changing from anisotropy to isotropy with fixed fiber distributions described in the literature. On the other

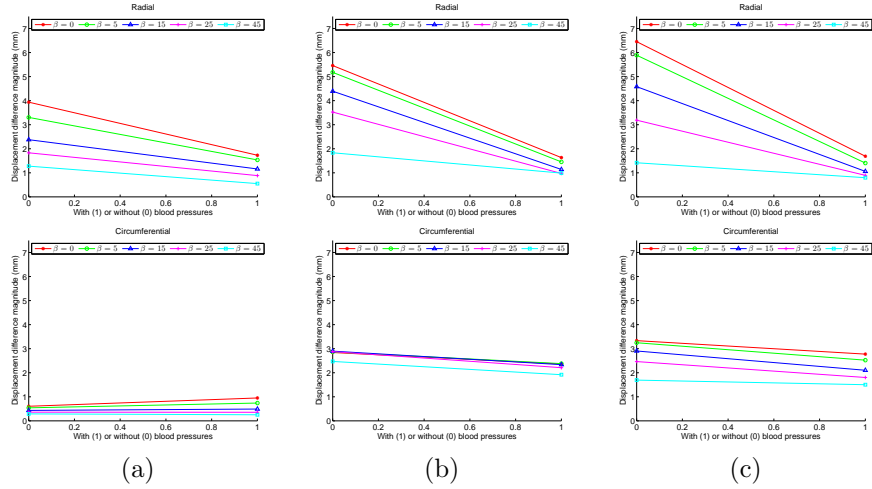


**Fig. 7.** Displacement difference magnitude versus with or without blood pressures, at the end of systole. (a) Synthetic data. (b) Patient data set 1. (c) Patient data set 2. Different colors encode different values of the image force scaling parameter  $\beta$ .

hand, the recovery framework is more sensitive to the active forces and the fiber orientations. In fact, the fiber orientations mainly impact two aspects of the model: the active contraction forces and the passive anisotropic mechanical properties. Although the results already showed that the ProActive Deformable Model is less sensitive to the stiffness anisotropy, we performed additional experiments with different fiber orientations without active forces. As it is meaningless to perform tests without both image and active forces, tests with  $\beta = 0$  (no image forces) were not performed. Fig. 6 shows that without active forces, the changes of the recovery results versus the changes of fiber orientations are ignorable. Thus if active forces are not used, passive isotropic mechanical models might be enough for motion estimation. Furthermore, the ranges of the displacement difference magnitudes are larger when using active forces, which means that proper active forces are very important for accurate motion recovery.

Fig. 7 shows the test results with or without using blood pressures as boundary conditions. The absence of blood pressures can lead to large deviations in the radial direction, but these deviations decrease with the increase of the image forces. On the other hand, the effects of the blood pressures are less obvious in the circumferential direction. This shows that blood pressure constraints are important when image information is not reliable, but strong image information as boundary conditions can compensate for improper blood pressure specifications.

The red lines in the plots correspond to the absence of image forces, so they provide an objective evaluation of the simulation accuracy of the ProActive Deformable Model through the *in vivo* patient data. As the in-plane resolutions are between 1.42 and 1.56 mm/pixel, the minimum displacement difference magni-

tudes in the pure simulations are between one and two pixels. This shows that the model can reproduce patient-specific cardiac deformation when the parameters are properly adjusted.

## 4 Conclusion

From the above discussions, we conclude that the cardiac motion recovery framework is less sensitive to the anisotropy of the passive biomechanical model, and is more sensitive to active forces, fiber orientations, and blood pressures, especially when image information does not provide strong constraints. Therefore, if reliable image information can be extracted, the framework can correctly track cardiac motion up to pixel size even with parameters taken from the literature (cyan lines). On the other hand, if image quality is low, *a priori* information from the electromechanical model is crucial and subject-specific fiber orientations and blood pressures should be estimated from available measurements. Recent progress on *in vivo* diffusion tensor imaging of the heart and pressure estimation from flow data can complement very well such approaches. Furthermore, the cardiac motions recovered from the synthetic images using the ProActive Deformable Model are very close to the simulated ground truth of the nonlinear electromechanical model. This means that even the biomechanical model used is linear, the recovery framework can provide useful patient-specific cardiac motions for parameter estimations of nonlinear models, which can help to predict patient-specific cardiac functions for surgical planning or treatments.

## References

1. Sermesant, M., Delingette, H., Ayache, N.: An electromechanical model of the heart for image analysis and simulation. *IEEE Transactions on Medical Imaging* **25**(5) (2006) 612–625
2. Wong, K.C.L., Zhang, H., Liu, H., Shi, P.: Physiome-model-based state-space framework for cardiac deformation recovery. *Academic Radiology* **14**(11) (2007) 1341–1349
3. Sundar, H., Davatzikos, C., Biros, G.: Biomechanically-constrained 4D estimation of myocardial motion. In: *International Conference on Medical Image Computing and Computer Assisted Intervention*. Volume 5762 of LNCS., Springer (2009) 257–265
4. Nash, M.: *Mechanics and Material Properties of the Heart using an Anatomically Accurate Mathematical Model*. PhD thesis, The University of Auckland (1998)
5. Niederer, S., Rhode, K., Razavi, R., Smith, N.: The importance of model parameters and boundary conditions in whole organ models of cardiac contraction. In: *International Conference on Functional Imaging and Modeling of the Heart*. Volume 5528 of LNCS., Springer (2009) 348–356
6. Sermesant, M., Konukoğlu, E., Delingette, H., Coudière, Y., Chinchapatnam, P., Rhode, K.S., Razavi, R., Ayache, N.: An anisotropic multi-front fast marching method for real-time simulation of cardiac electrophysiology. In: *International Conference on Functional Imaging and Modeling of the Heart*. Volume 4466 of LNCS., Springer (2007) 160–169

7. Ourselin, S., Roche, A., Prima, S., Ayache, N.: Block matching: a general framework to improve robustness of rigid registration of medical images. In: International Conference on Medical Image Computing and Computer Assisted Intervention. Volume 1935 of LNCS., Springer (2000) 557–566
8. Sainte-Marie, J., Chapelle, D., Cimrman, R., Sorine, M.: Modeling and estimation of the cardiac electromechanical activity. *Computers and Structures* **84** (2006) 1743–1759
9. Toussaint, N., Mansi, T., Delingette, H., Ayache, N., Sermesant, M.: An integrated platform for dynamic cardiac simulation and image processing: application to personalised tetralogy of fallot simulation. In: Eurographics Workshop on Visual Computing for Biomedicine (VCBM). (2008)
10. Cerqueira, M.D., Weissman, N.J., Dilsizian, V., Jacobs, A.K., Kaul, S., Laskey, W.K., Pennell, D.J., Rumberger, J.A., Ryan, T., Verani, M.S.: Standardized myocardial segmentation and nomenclature for tomographic imaging of the heart: a statement for healthcare professionals from the cardiac imaging committee of the council on clinical cardiology of the American Heart Association. *Circulation* **105** (2002) 539–542